13th World Conference on Earthquake Engineering
Vancouver, B.C., Canada
August 1-6, 2004
Paper No. 587

APPLICATION OF INTENSIVE SHEAR REINFORCEMENT TO SPLICING SLEEVE JOINT OF PRE-FABRICATED REINFORCEMENT ASSEMBLY

Katsumi KOBAYASHI[1], Masato ISO[2], Yasuhiro MATSUZAKI[3], Masaaki ASE[4]

SUMMARY

Heavy shear reinforcement is intensively placed at the ends of splicing sleeve joint in PCa members. This is called Intensive Shear Reinforcement (ISR). It was presented at 11WCEE that the shear reinforcement in the splicing sleeve zone could be removed when ISR is arranged. If ISR is placed in addition to the regular shear reinforcement, both shear capacity and splitting bond capacity increase, and as a result the ductility increases. The test results were presented at 12WCEE. In this paper, ISR was placed at the ends of the splicing sleeve joint of pre-fabricated reinforcement assembly in order to compensate no-bond resistance on the sleeve surface. RC beams with splicing sleeve joint in mid span were tested. The splitting bond capacity increased, even if the bond resistance was removed from the sleeve surface. The compression force acting at the end of the sleeve forms a truss mechanism in cooperation with ISR and diagonal concrete strut, and it effectively compensates no-bond resistance on the sleeve surface. A design recommendation to determine the amount of ISR was proposed on the basis of the analytical model. A larger amount of ISR increases both splitting bond capacity and shear capacity. The evaluation method for capacities was also discussed using a modified strut-tie model.

INTRODUCTION

When introducing a mechanical splicing joint, it may be difficult to expect bond resistance depending on the surface condition of a splicing unit and to secure the bond length of the longitudinal bars. It is thought that the bond resistance may not be expected in case of the splicing sleeve joint. On the other hand, it is thought that it can be expected because the splicing sleeve has a large circumference and roughness on the surface. In addition it has the grouting holes that will work as dowels against concrete. However, the bond resistance can hardly be expected in such a case of splicing coupler with smooth surface for screw bars.

[1] Professor, University of Fukui, Fukui, Japan. Email: katsumi@anc.anc-d.fukui-u.ac.jp
[2] Assistant Professor, University of Fukui, Fukui, Japan. Email: iso.masato@anc.anc-d.fukui-u.ac.jp
[3] Professor, Science University of Tokyo, Tokyo, Japan. Email: ymatsu@rs.kagu.sut.ac.jp
[4] Director, Splice Sleeve Japan, Tokyo, Japan. Email: ase@splice.co.jp

There are few problems if the splicing joints locate in the region of "d" from the member end (d: effective depth of section) in such a case of PCa columns. The length in this region is excluded from the calculation of bond length. It is calculated from the point that is far from the member end by "d" in the current design standard, AIJ [2]. It becomes difficult to secure the bond length if the bond resistance on the surface of splicing unit cannot be expected, when the mechanical splicing joint locates on the mid-span of member with pre-fabricated reinforcement assembly, or when it locates in the beam-column connection in PCa moment resisting frame system. This paper will propose a method to calculate the bond length including the region of splicing joint by providing ISR at both side of splicing unit. It is no need to expect the bond resistance on the surface of the splicing unit. The proposed theory was verified with the experiment of RC beams with splicing joint on the mid-span of beam. The intensive shear reinforcement (ISR) is defined as shear reinforcement with large size bar or a bundle of shear reinforcement with normal size bar that is placed at both sides of splicing unit.

APPLICATION OF INTENSIVE SHEAR REINFORCEMENT

Bending-shear crack occurs at the member end and a tension shift takes place. Furthermore, the tensile force distribution on the main bar becomes as shown in Fig. 1 and the bond length is reduced, if the bond resistance on the surface of splicing unit cannot be expected. The design for bond resistance may become difficult, according to the current design standard, AIJ [2]. A mechanical splicing unit has a larger section comparing with the main bar. The difference of tensile force of main bar at both ends of splicing unit ($T_1 - T_2$) will be allowed if the reaction force from the concrete can be expected at one end of splicing unit, though the bond resistance is not expected on the surface of splicing unit as shown in Fig. 2. At the member end, the reaction force R_2 is not expected because there occurs bending crack. Then a vertical force is required, that balances with the vertical component of reaction force R_1. The shear reinforcement will work to carry this vertical force, but the amount is too small to balance the vertical component of R_1. If ISR is placed here, it can carry a large force that balances the vertical component of R_1. ISR has to balance with the difference of tensile force of main bar too, that is equivalent to the bond resistance in the length of splicing unit. If it works effectively, it may be possible to calculate the bond length including the region of splicing joint seemingly, as shown in Fig. 3, in the same way as in a member without mechanical splicing joints.

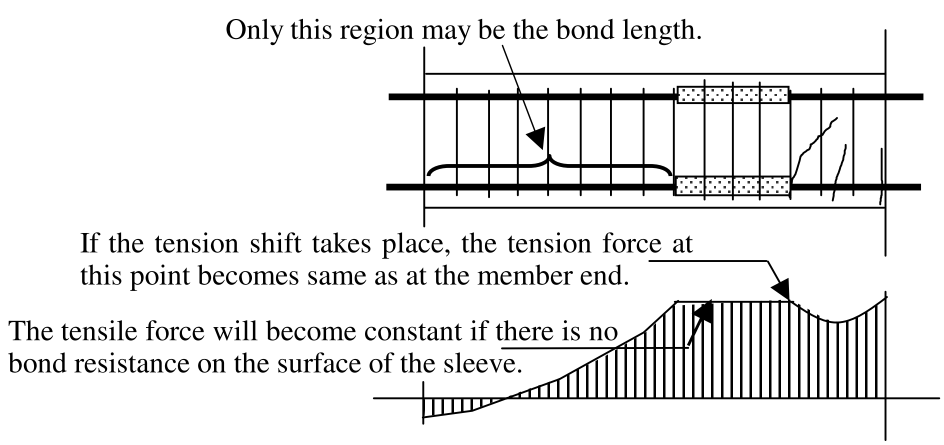

Fig. 1 Tensile force distribution where there is no bond resistance on the sleeve

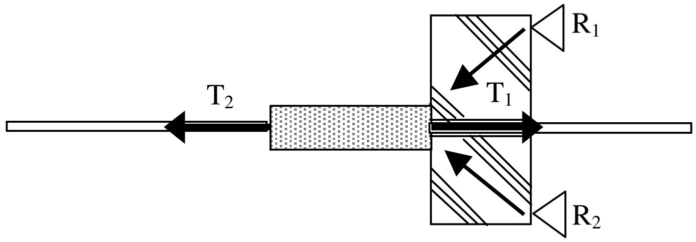

Fig. 2 Equilibrium of forces at the end of sleeve expecting the bearing stress

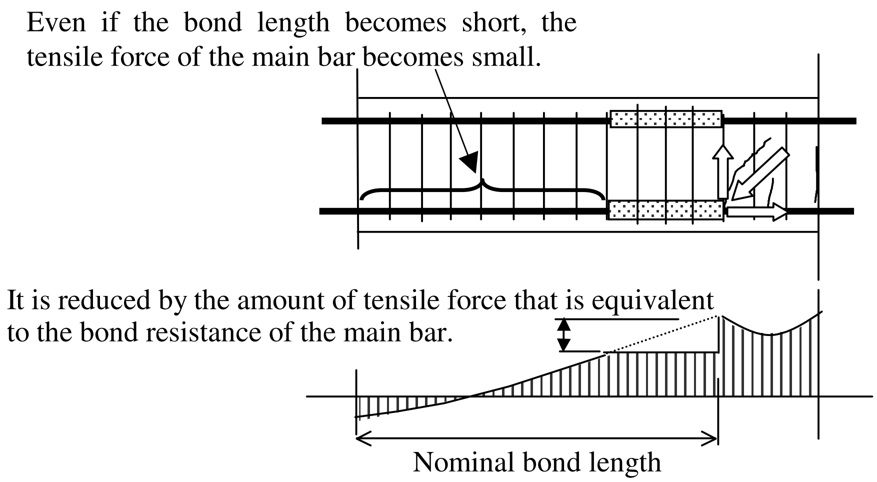

Fig. 3 Tensile force distribution when ISR is placed

EXPERIMENTAL PROGRAM

Three specimens shown in Fig. 4 were tested. RC-32S is the control specimen and has no splicing joints. The section size ($B \times D$) is 250x300mm. The shear span to depth ratio (a/D) is 2.0. Three main bars of D19 were placed in both tensile and compressive side. The transverse reinforcement of D6 was placed at the interval of 80mm. The shear reinforcement ratio (p_w) is 0.32%. The ratio of shear capacity calculated by a strut-tie model by AIJ [3] to flexural capacity is 0.85. The ratio of the bond strength of main bar by AIJ [3] to the design bond stress ($d_b \cdot 2\sigma_y /(L-d)$) is 0.63. It was scheduled that the splitting bond failure might precede. IS00-32S has splicing joints at the distance of 275mm from the beam end, and the tensile force distribution on main bar shown in Fig. 1 was expected. IS16-32S has ISR, and the tensile force distribution on main bar shown in Fig. 3 was expected. A bundle of two round bars of 16mm in diameter were used as ISR. The shape of splicing sleeve unit is shown in Fig. 5. To remove the bond resistance on the surface of splicing sleeve, all the projections such as the grouting holes were scraped off, and completely smooth cylindrical sleeves were prepared. Paraffin wax was put on the surface of splicing sleeve and furthermore, the surface was wrapped with vinyl tape. The mechanical properties of materials are listed in Table 1. The loading system is illustrated in Fig. 6. The reversed cyclic loads were given gradually increasing the drift angle so that the mid-span has a reversed symmetrical moment distribution. The strain of main bars, shear reinforcement and ISR was measured with strain gages.

Table 1 Mechanical properties of materials

Concrete (Age: 70 days)			Steel bars			
Compressive Strength σ_B (MPa)	Young's Modulus $_C E$ (GPa)	Splitting Tensile Strength σ_t (MPa)		Yield Strength σ_y (MPa)	Tensile Strength σ_m (MPa)	Young's Modulus $_S E$ (GPa)
25.7	19.9	1.88	D19	602	797	200
Grout mortar (Age: 98 days)			D6	343	519	172
90.4			ϕ 16	301	444	207

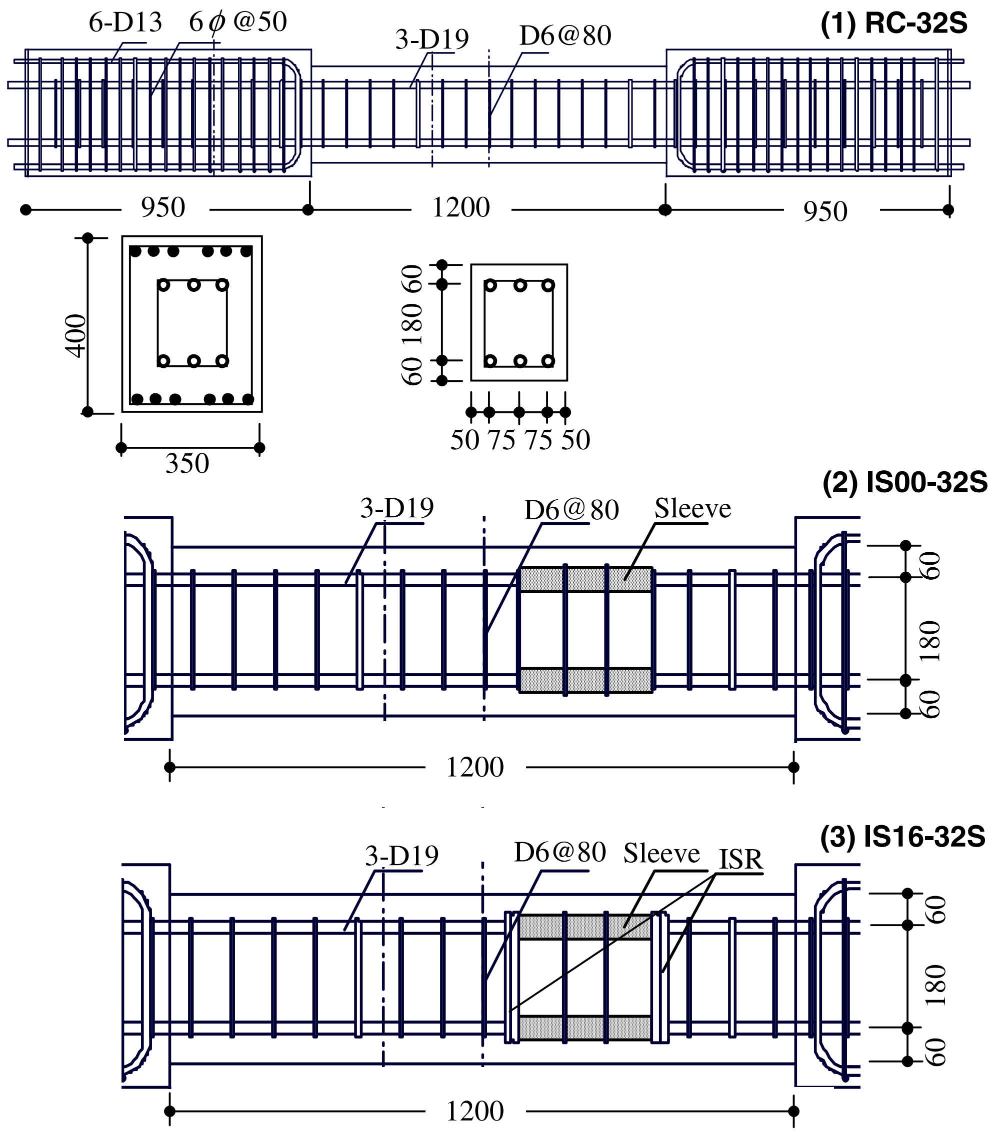

Fig. 4 Specimens

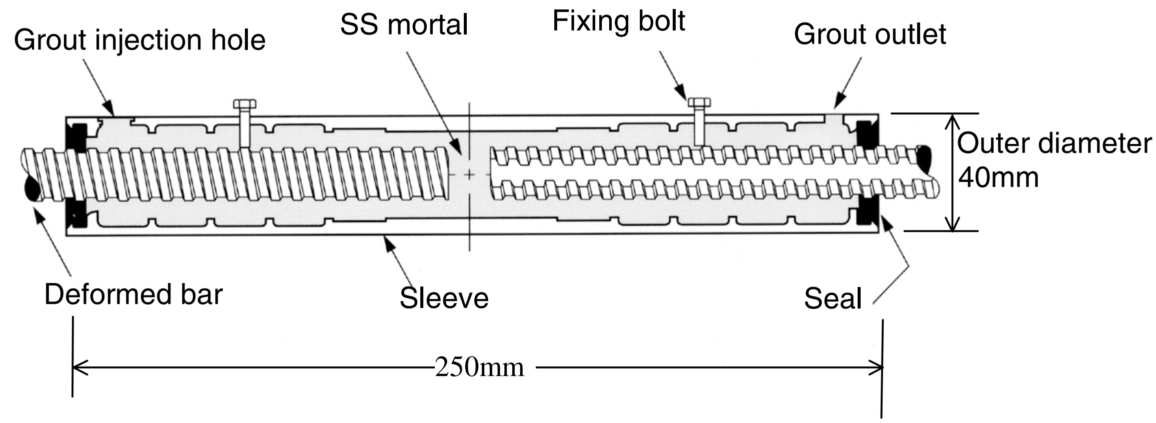

Fig. 5 Shape of splicing sleeve

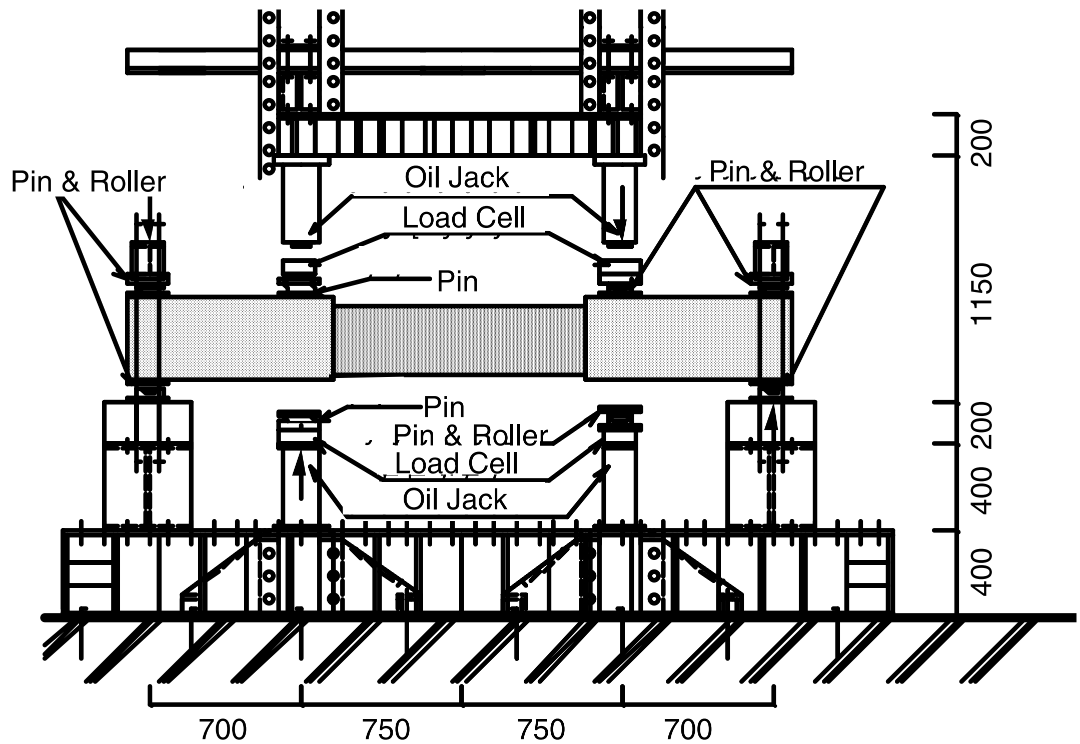

Fig. 6 Loading apparatus

TEST RESULTS

Shear force - relative displacement relationship

Shear force - relative displacement relationships are shown in Fig. 7. The specimen, IS00-32S with splicing joints showed almost same capacity as the control specimen, RC-32S. There was no difference in the hysteretic loops after the maximum shear force. It is supposed to be a reason that both IS00-32S and RC-32S failed in splitting bond failure mode. The maximum shear force increased in the specimen, IS16-32S with ISR at both ends of splicing sleeve. The bearing force dropped down quickly at the drift angle of 1/200. This was more affected by shear cracks rather than splitting bond cracks.

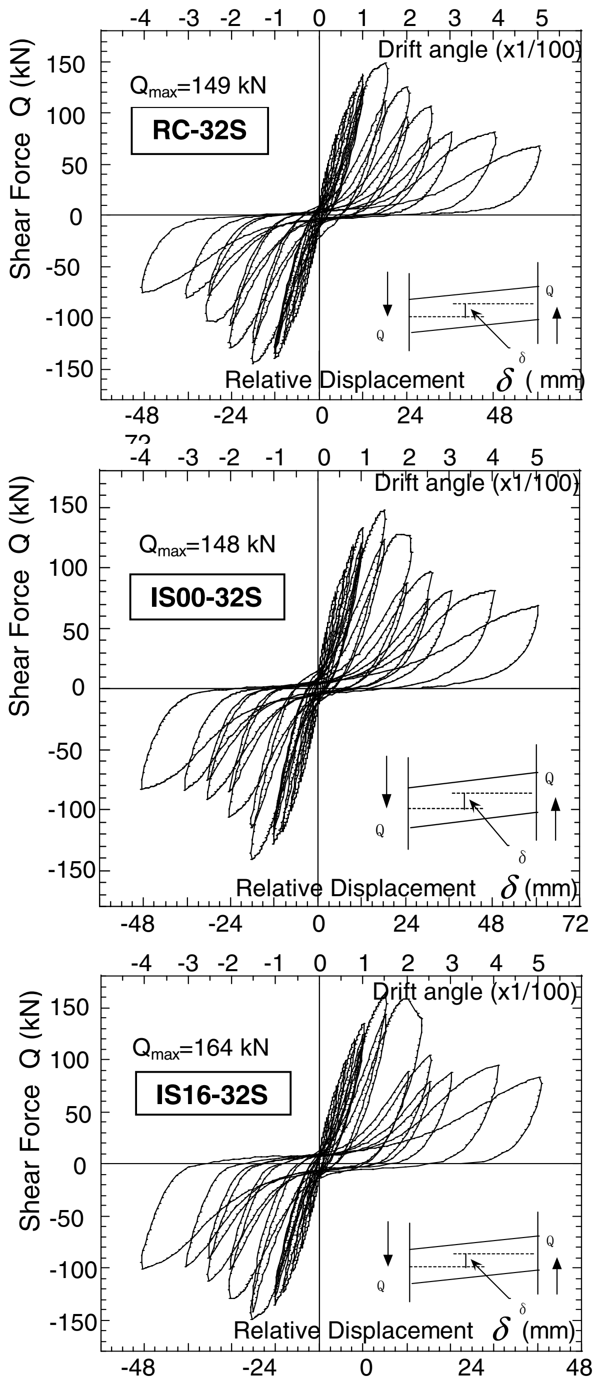

Fig. 7 Shear force-relative displacement relations

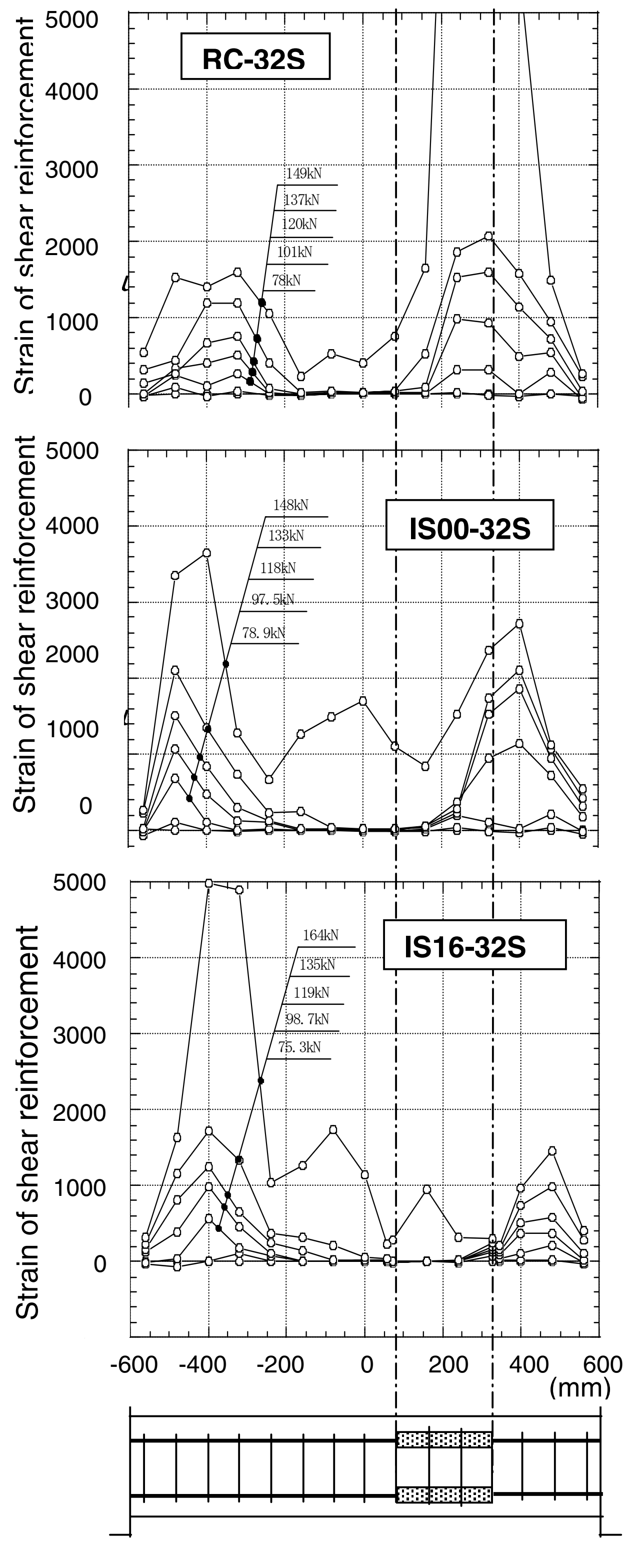

Fig. 8 Strain distribution on shear reinforcement

Strain on the shear reinforcement

The measured strain on the shear reinforcement is shown in Fig. 8. The yield strain of shear reinforcement, D6, was about 0.2%. In the control specimen, RC-32S, shear reinforcement at both ends of beam showed large strain, and it exceeded the yield strain at right hand side at the ultimate state. In the mid-span of the specimen, the strain of shear reinforcement was small. However, in the specimen, IS00-32S with splicing joints, the strain of shear reinforcement at both ends of beam exceeded the yield strain at the ultimate state. The strain got large at mid-span too. This corresponded to the cracking pattern, which was different from that of the control specimen, and the shear crack that occurred at mid-span. In the specimen, IS16-32S with ISR at both sides of splicing sleeve, the strain of shear reinforcement got large and exceeded the yield strain at one side of the beam where there is no splicing sleeve. It showed a pattern in which the distribution in IS00-32S was squeezed at both sides of splicing sleeve. The strain at both sides of splicing sleeve is 100 to 150 μ. To keep this strain small is essential, and it changes the cracking pattern, and it is supposed to be one condition that gives guarantee to the mechanism described in this paper.

Cracking behavior at the maximum load

The crack pattern at the maximum load is shown in Fig. 9. Bending-shear cracks occurred at both ends of the control specimen, RC-32S. They correspond to the fact that the strain of shear reinforcement at both sides of the beam was large. Although it is difficult to distinguish the shear failure and the splitting bond failure clearly, it is judged that the maximum load was determined by the bond failure since much bond cracks were observed long the main bar at the maximum load. The specimen, IS00-32S with splicing joints has less bond cracks compared with the control specimen, RC-32S, and it has a shear crack at mid-span. It corresponds to the fact that the strain of shear reinforcement at mid-span became large. However, this shear crack did not trigger the failure, and the maximum load is supposed to be governed by the influence of bond. The specimen, IS16-32S with ISR at both sides of splicing sleeve, has extremely few cracks compared with the specimen, IS00-32S without ISR. A shear crack at mid span is clear. The number of bond cracks has decreased and the influence of bond is removed. Because of the existence of ISR, the region of splicing joint becomes rigid and it is supposed to generate few cracks. A cracking pattern was observed as if the shear span to depth ratio was reduced. Although the maximum load only increased by about 10%, the stress transfer mechanism may be changing a lot, compared with the control specimen, RC-32S, and the specimen, IS00-32S without ISR.

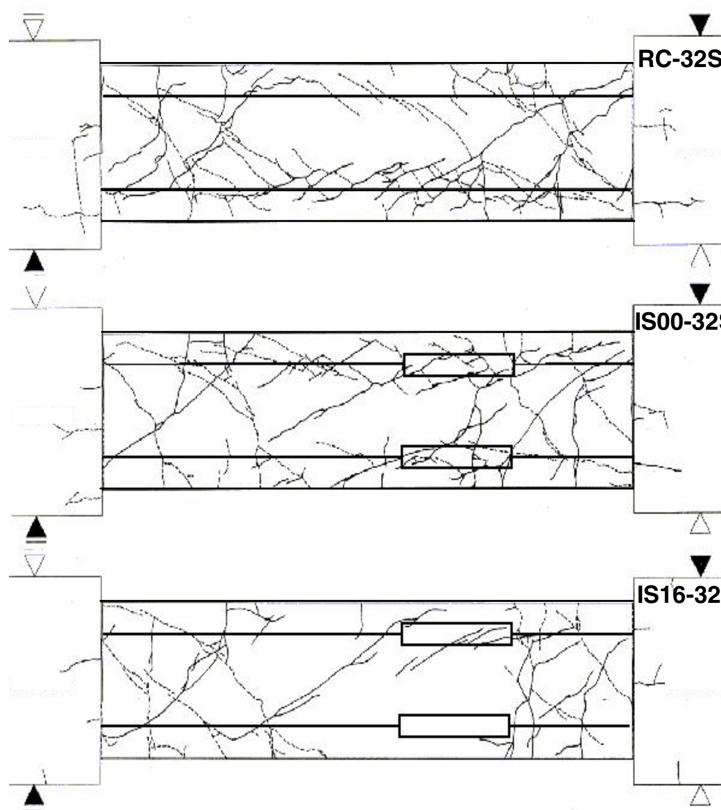

Fig. 9 Cracking pattern at the maximum load

Tensile force distribution on the main bar

The measured strain distribution on the main bar is shown in Fig. 10. The main bar did not yield in all specimens. Therefore, a strain distribution is the same as a tensile force distribution. The complete tension shift at the end of the specimen has not taken place in all the specimens. Bending and shear crack was generated. As shown in Fig. 11, however, the difference of tensile force on the right and the left of the main bar may be allowed if the tensile force of shear reinforcement balances with the tensile force of the main bar, because there is bond resistance on the main bar in the region between the cracks. Figure 12 shows the left and the right hand side of a formula indicated in Fig. 11 based on the measured strain of the control specimen, RC-32S. ΔT is the difference of tensile force which was calculated from the measured strain in Fig. 10. j is the rotational radius when assuming the rotational center is at the position of the compressive main bar. j was assumed to be 18cm in Fig. 12. The equilibrium of forces shown in Fig. 11 is verified from the result of Fig. 12.

IS00-32S shown in Fig. 10 has splicing sleeves of which bond resistance was removed, and has no ISR. The strain of main bar at both ends of splicing sleeve is almost same, and it coincides with the tensile force distribution schematically illustrated in Fig. 1. IS16-32S shown in Fig. 10 has splicing sleeves of which bond resistance was removed, and ISR was placed. There was a difference of strain of main bar at both ends of splicing sleeve. It was similar to that of the control specimen without splicing joints. It coincides with the tensile force distribution schematically illustrated in Fig. 3 that was expected for the specimen with ISR.

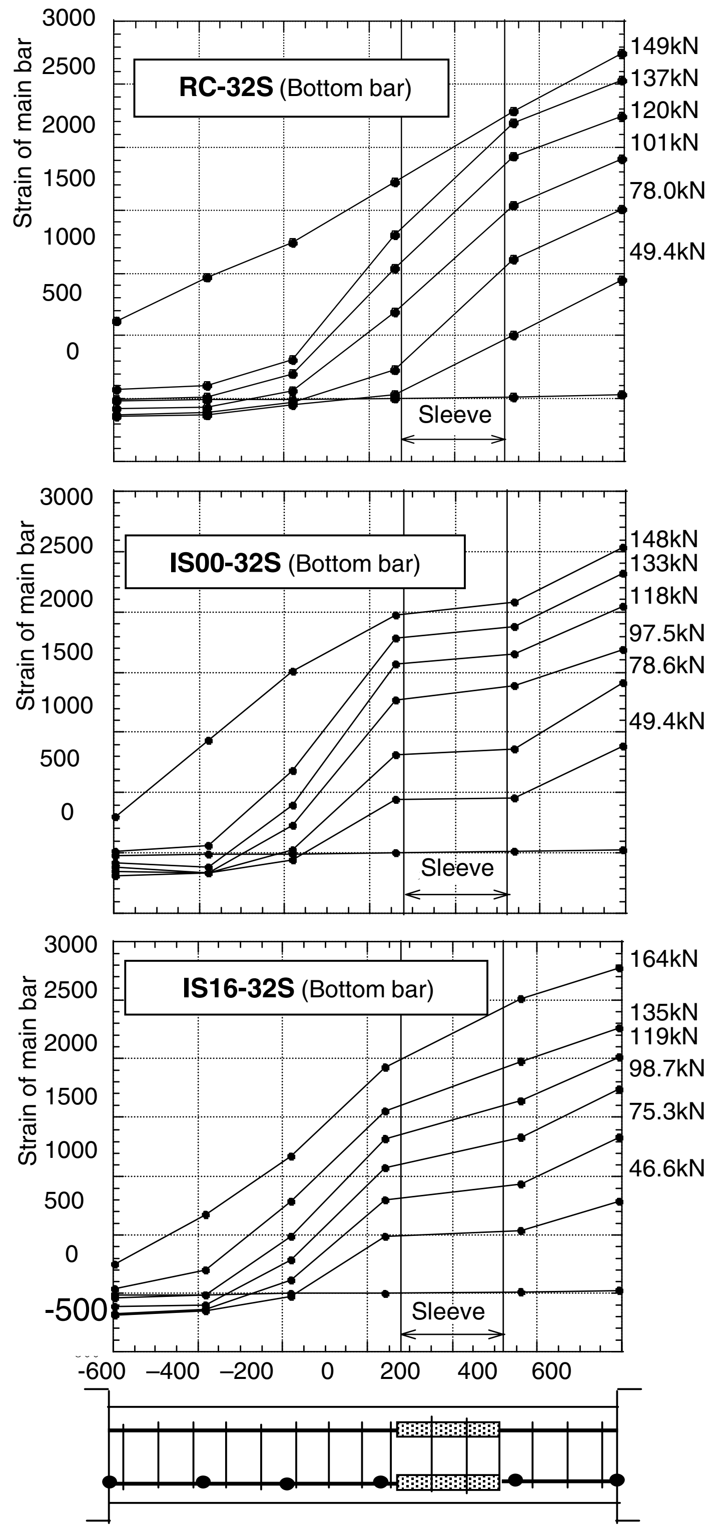

Fig. 10 Strain distribution on main bar

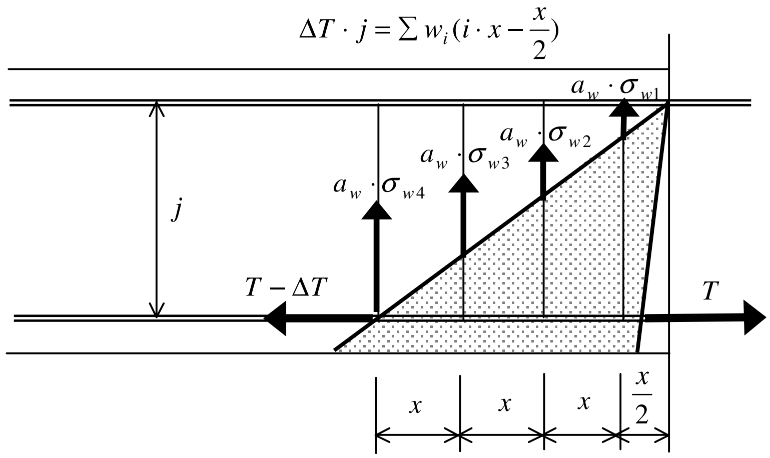

Fig. 11 Tensile force distribution at the end of member

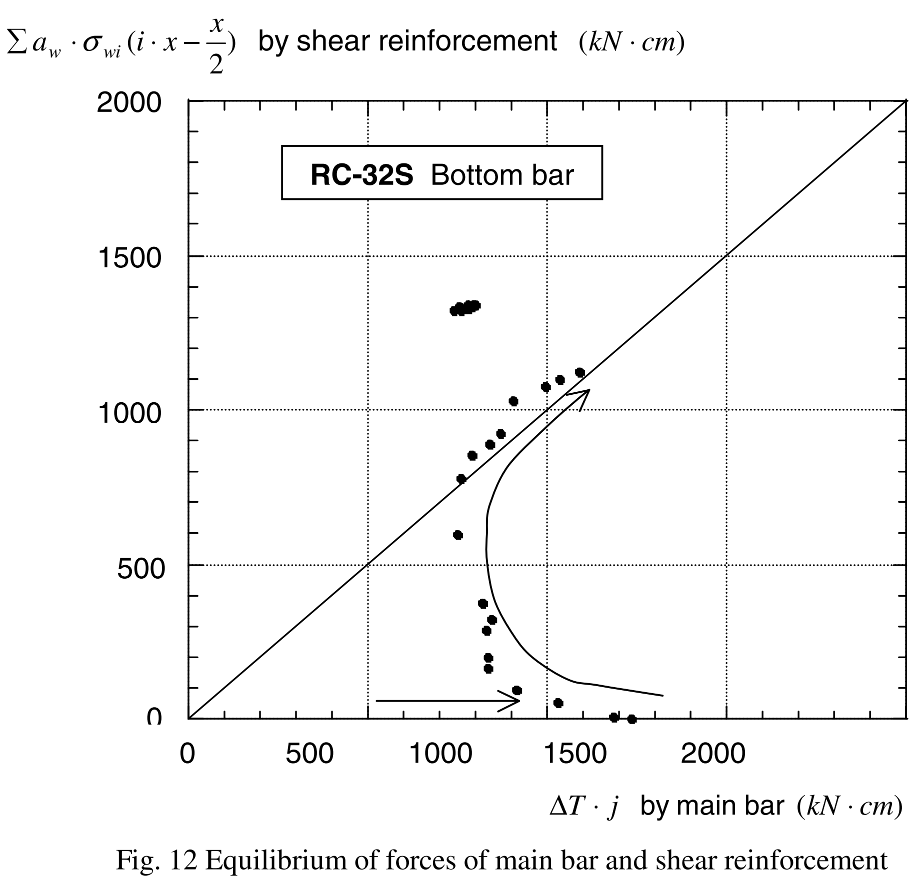

Fig. 12 Equilibrium of forces of main bar and shear reinforcement

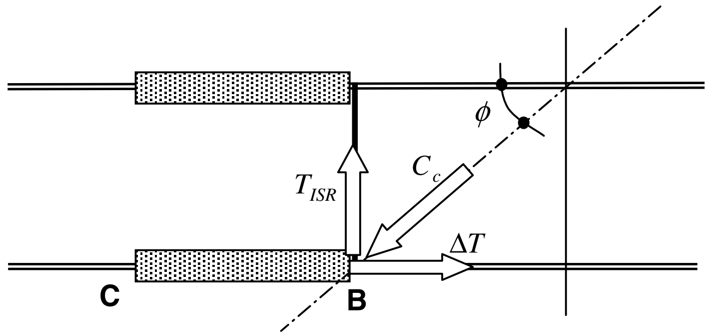

Fig. 13 Equilibrium of forces by ISR

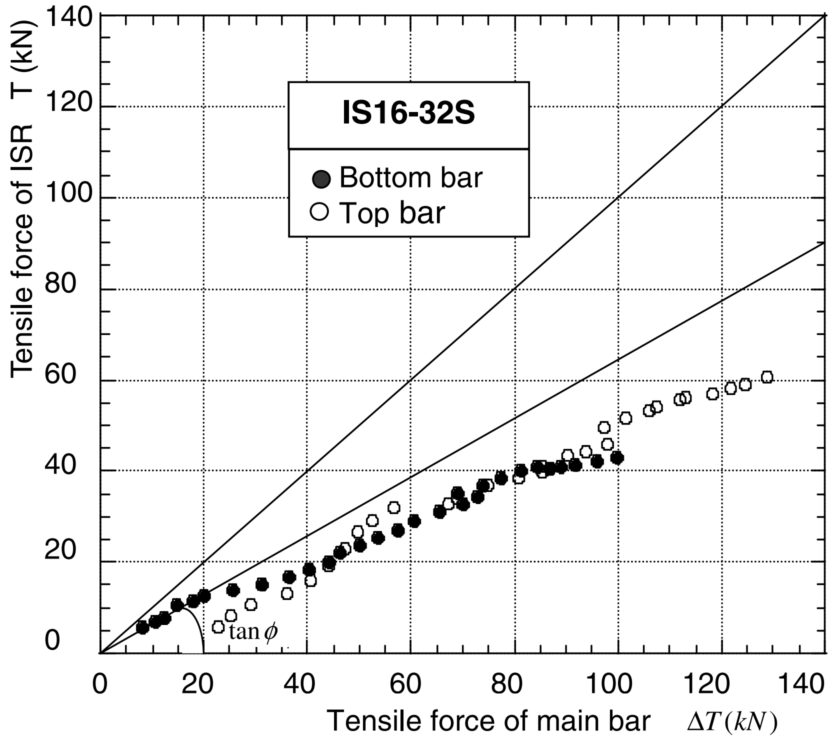

Fig. 14 Measured tensile forces of ISR and the main bar

TENSILE FORCE OF MAIN BAR AT BOTH ENDS OF SPLICING SLEEVE AND TENSILE FORCE OF INTENSIVE SHEAR REINFORCEMENT

The equilibrium of forces shown in Fig. 3 is illustrated again in Fig. 13. The difference of tensile force between the point B and the point C (ΔT), the tensile force of ISR (T_{ISR}) and the compression force of concrete strut (C_c) are balanced. When the angle of concrete strut is defined ϕ, the ratio of T_{ISR} to ΔT must be $\tan\phi$. In the specimen tested in this study, ISR restrains only the main bars on the corner of the section directly, and the tensile force of the inner main bar and the compression strut must balance with ISR through concrete. Ideally it is better for all main bars to be restrained by ISR. However, it is judged that the equilibrium shown in Fig. 13 was almost achieved, since the rigidity of ISR is comparatively large and the interval of splicing sleeves side by side is 35mm. It is unresolved and a future research topic whether the equilibrium of forces shown in Fig. 13 can be achieved with what interval of splicing sleeves side by side. Figure 14 is the relation between ΔT and T_{ISR} of the specimen, IS16-32S shown in Fig. 4. ΔT was calculated from the difference of the measured strain of main bar at both sides of splicing sleeve (The difference of the measured strain of an inner main bar was multiplied by the sectional area of three main bars and Young's modulus.). Strain measurement positions are the both sides of splicing sleeve shown in Fig. 10. T_{ISR} was calculated from the measured strain of ISR (ISR was made of two round bars of 16mm in diameter. The strain gages were installed on two round bars in front and two round bars another side. The average strain of four bars was multiplied by sectional area of the four bars and Young's modulus.). The inclined solid line in Fig. 14 shows the ratio of T_{ISR} to ΔT assuming the concrete strut orients the position of compressive main bar at member end. The plotted experimental results are close to this line, and they will come more close to this line if the tensile force of regular shear reinforcement is added to T_{ISR}. The equilibrium of forces in Fig. 13 is well verified from the results in Fig. 14.

CALCULATION FOR THE AMOUNT OF INTENSIVE SHEAR FREINFORCEMENT

The intended tensile force distribution on the main bar for the structural design for the bond resistance is shown in Fig. 15. The difference of the tensile force (ΔT) at both ends of splicing sleeve is figured out. The amount of ISR can be calculated on the basis of the equilibrium of forces illustrated in Fig. 13. In order to guarantee the stress distribution on the main bar shown in Fig. 15,

$$T_{ISR} = \Delta T \cdot \tan\phi \tag{6.1}$$

$$\Delta T = 2\sigma_y \cdot a_r \cdot l_s /(l-d) \tag{6.2}$$

Here, a_r is the sectional area of a main bar. The splicing joints are assumed to locate at the distance of d (effective depth of section) from the member end. The angle of the concrete strut ϕ is assumed to orient the position of the compressive main bar at member end.

$$a_{ISR} = 2\sigma_y \cdot a_r \cdot l_s \cdot \tan\phi /(l-d)/\sigma_{ISR} \tag{6.3}$$

Here, a_{ISR} is the sectional area of ISR. σ_{ISR} is the expected stress of ISR. The horizontal component of concrete strut acts on the end of splicing sleeve as the bearing stress, and balances with ΔT. Therefore, ΔT depends on the bearing stress intensity of concrete.

$$\Delta T \le A_{LC} \cdot f_{LC} \tag{6.4}$$

A_{LC}: Effective bearing area at the end of sleeve
f_{LC}: Bearing stress intensity of concrete

f_{LC} may be expected to be about 2.0 F_c (F_c: Specified concrete strength) according to the standard for prestressed concrete structures, AIJ [4]. However, it is unsolved how much bearing stress intensity can be expected. It will be a research topic in the future. The splicing sleeve has a sealing material made of rubber at the both ends, and just the net area of the cylindrical sleeve may receive the bearing stress. However, it may be a possibility that the area including the sealing material is evaluated as bearing area,

when considering the stress condition inside the concrete that receives the bearing stress distributing on circumference. Also a large bearing stress on the side of ISR may be expected, that is placed at the end of splicing sleeve. Matagari [5] confirmed a large bearing stress at the end of splicing sleeve in his test program, and it will be a research topic in the future how much is the bearing area as well as how much is the bearing stress intensity.
From Eq. (6.4) and Eq. (6.1),

$$T_{ISR} \leq A_{LC} \cdot f_{LC} \cdot \tan\phi \qquad (6.5)$$

$$a_{ISR} \leq A_{LC} \cdot f_{LC} \cdot \tan\phi / \sigma_{ISR} \qquad (6.6)$$

From Eq. (6.6), the upper limit of the amount of ISR is obtained. However, if the amount of ISR (a_{ISR}) increases over the limit, the elongation of ISR decreases, and it works advantageously against shear and bond failure. On the other hand, is it possible to reduce the area of ISR by using high strength materials? The equilibrium of forces illustrated in Fig. 13 may not be guaranteed, because the elongation of ISR increases too much. If this is taken into consideration, the lower limit of the amount of ISR will be determined. The elongation of ISR depends on the bond with concrete and its shape. It will be difficult to figure out the limit by calculation. The experimental approach will have to be used to determine it in the future. It is afraid that ISR cannot demonstrate a large tensile force although it has enough large sectional area, if its position is separated from the end of splicing sleeve or it does not touch the main bar tightly as Koyama [6] gives a warning. The detail of ISR must be well considered.

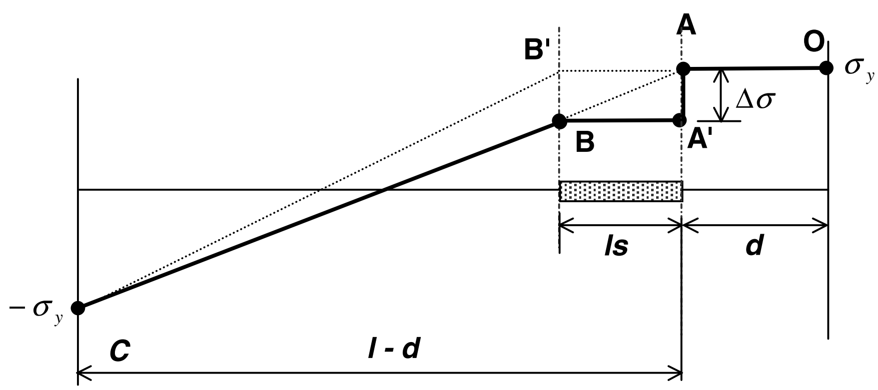

Fig. 15 Tensile force distribution on the main bar for design

SPLITTING BOND CAPACITY

In case that there is no bond resistance on the surface of splicing sleeve (IS00-32S), an expected tensile force distribution was observed, where the region of splicing joint could not be included in the bond length. However, the splitting bond capacity is not different from that of the specimen without splicing joints as shown in the shear force-displacement relations in Fig. 7. In the specimen with ISR at the both ends of splicing sleeve (IS16-32S), the nominal bond length may be calculated in the same way as in the specimen without splicing joints (RC-32S). However, the splitting bond capacity increased by about 10%. Figure 13 shows equilibrium of forces at one side of splicing joints, and a similar equilibrium of forces must exist at another side as illustrated in Fig. 16. The shear force transfer mechanism in the region of splicing joints is complicated. However, the cracking pattern and the angle of cracks of IS16-32S shown in

Fig. 9 correspond to forces illustrated in Fig. 16. It is understandable that ISR work as a normal shear reinforcement and the shear capacity will increase. In addition, when a strut-tie model (truss-arch mechanism) is applied to evaluate the splitting bond capacity, the concrete strut is thought to bend and its angle becomes steeper as shown in Fig. 16, and eventually the splitting bond capacity increases. Furthermore, the main bars are confined by ISR and pressed on the concrete, and then the friction will increase a lot around ISR. Even in a specimen, IS00-32S without ISR, a shear crack occurred at mid-span. It is supposed that the normal shear reinforcement would work like ISR. It positively leads to the splitting bond capacity gain, and it is supposed to compensate the decrease of splitting bond capacity due to the reduction of bond length.

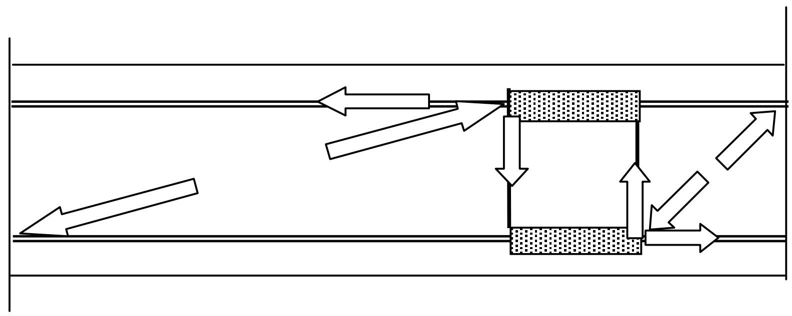

Fig. 16 Arch action produced by ISR

CONCLUSION

A design concept for the bond resistance of mechanical splicing joint was proposed. If ISR is provided, the bond length can be evaluated including the region of splicing joint even if there is no bond resistance on the surface of splicing unit. The mechanism was verified by experiment and the effectiveness of arranging ISR was confirmed. It needs to verify the proposed design concept by experiment with a larger model in the future.

REFERENCES

1. Ikadai F, Kobayashi K, Ase M, Abukawa M. “Bond Behavior in PCa Columns with Mortar Grouted Sleeve Joint.” Proceedings of the Japan Concrete Institute, Vol.21, No.3, 1999: 805-810
2. “AIJ Standard for Structural Calculation of Reinforced Concrete Structures.” Architectural Institute of Japan, 1999
3. “Design Guidelines for Earthquake Resistant Reinforced Concrete Buildings Based on Ultimate Strength Concept.” Architectural Institute of Japan, 1990
4. “Standard for Structural Design and Construction of Prestressed Concrete Structures.” Architectural Institute of Japan, 1998
5. Matagari K, Ase M, Minami K. “Experiment on the Bond of Reinforcement Including Splice Sleeve (Part 1).” Summaries of Technical Papers of AIJ Annual Meeting, C-2, 2001: 133-134
6. Koyama A, Takagi H, Kanoh Y. “Experimental Study on Ductility Capacity of Precast Concrete Columns Connected by Sleeve-joints with Intensive Shear Reinforcing.” Summaries of Technical Papers of AIJ Annual Meeting, C-2, 1996: 757-758